Department of Electrical and Computer Engineering
North South University

Senior Project Design

All object on-chip tractor beam using SPP

Team Members:

Name:	ID:
1. Masudur Rahim	132 0251 043
2. Md. Mohaimanul Masud Sunny	122 0446 043
3. Fahim Al Ifran Rahim	132 0650 043

Faculty Advisor:
Dr. Mahdy Rahman Chowdhury
Associate Professor
Department of Electrical and Computer Engineering
North South University

Fall 2020

Declaration

This is to declare that no part of this report or the project has been previously submitted elsewhere for the fulfillment of any other degree or program. Proper acknowledgement has been provided for any material that has been taken from previously published sources in the bibliography section of this report.

....

Masudur Rahim
Department of Electrical and Computer Engineering
North South University, Bangladesh

....

Md. Mohaimanul Masud Sunny
Department of Electrical and Computer Engineering
North South University, Bangladesh

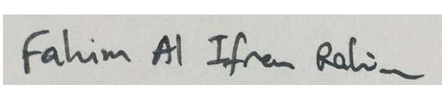

....

Fahim Al Ifran Rahim
Department of Electrical and Computer Engineering
North South University, Bangladesh

Approval

The Senior Design Project entitle "All object on-chip tractor beam using SPP" by Masudur Rahim, Md. Mohaimanul Masud Sunny and Fahim Al Ifran Rahim has been accepted as satisfactory and approved for partial fulfillment of the requirement of BS in EEE degree program.

MAHDY

……………………………………………………………………

Supervisor's Signature

Dr. Mahdy Rahman Chowdhury

Associate Professor

Department of Electrical and Computer Engineering

North South University

Dhaka, Bangladesh.

……………………………………………………………………

Dr. Mohammad Rezaul Bari

Associate Professor & Chair

Department of Electrical and Computer Engineering

North South University.

Dhaka, Bangladesh.

Acknowledgement

First of all, we would like to express our profound gratitude to our honorable course instructor, Dr. Mahdy Rahman Chowdhury, for his constant and meticulous supervision, valuable suggestions, his patience and encouragement to complete this research.

We would like to thank everybody who supported us and provided with guidance for the completion of this research.

Abstract

In this paper we designed an on-chip configuration where implementation of an all object optical tractor beam was made possible. By all object, we are referring to spherical nanoparticles of dielectric, plasmonic and chiral material. This tractor beam was composed of the superposition of two evanescently confined surface waves called SPP (Surface Plasmon Polariton), which was excited over the on-chip base by the incidence of a plane polarized laser light propagating vertically upwards. Arrays of nanoantenna like structures called metasurfaces has been used in this setup to manipulate the evanescent surface wave. Exerting pulling force is only possible when the beam incident over the particle has a non-paraxial nature. In reality, non-paraxiality of a beam is a somewhat hypothetical requirement. However, this issue is resolved by creating an interference field formed by the superposition of the SPP beam along with the induced effect within the particle and the substrate which led to the emergence of this backward pulling force. Pulling force was realized within certain diameter range (Mie Range). To the best of our knowledge, this article stands as the first proposal of realizing all object tractor beam in an on-chip configuration where the configuration itself is mitigating the paraxiality issue for all objects and using the same setup, pulling of such particles can be realized. Our work can be extended to sorting of particles in an inhomogeneous mixture, such as analysis of biomolecules.

Table of Contents

Chapter Page

List of figures

CHAPTER 1: INTRODUCTION

In 1619, Johannes Kepler proposed that it was the pressure of sunlight that blew back a comet's tail so that it always pointed away from the Sun. However, this remained only as a statement in that time as the science and technology in that time was not advanced enough to test such an issue. Then, in 1873 James Clarke Maxwell was able to shed some light into the issue as he theoretically proved that light waves indeed exert pressure and he wrote that "In a medium in which waves are propagated, there is a pressure in the direction of normal to the waves, and numerically equal to the energy in a unit of volume. Einstein proved that light has wave particle duality, meaning it behaves as a wave as well as a particle, which means that light incident upon any surface would cause bombardment of these particles over the surface thereby exerting a force in the particle that will be acting in the same direction as the direction of propagation of light. So, we can see that people had a good realization about the ability of light to exert radiation pressure. This was the normal ideology which follows all common norms of physics such as momentum conservation. Later on, in 1970, the discovery of optical tweezers opened up a new area of research where scientists worked on manipulating different parameters of the incident light to exert non-conservative force over the radiated object, where the illuminated object would have its resultant force in the direction opposite to the wave propagation of the incident beam, which scientists named optical-tractor beam. The optical tweezer was developed into a powerful tool for the manipulation of micro-objects and biomolecules that was used in different fields of science for the analysis of biomolecules, sorting, trapping and binding of particles in the microscale or nanoscale etc. Such optical manipulation methods have become important research tools, with wide-ranging applications in biology and biomedicine, microfluidics and colloidal science. More recently, there has been a growing interest in levitation dynamics in optomechanical systems, including passive and active feedback schemes, for realizing quantum mechanical superposition, ground-state cooling and coherent manipulation of mechanical systems.

In this research work, we work on surface wave tractor beams which have drawn less attention compared to free-propagating optical tractor beams. Surface plasmon polaritons (SPPs) are electromagnetic excitations propagating at the interface between a dielectric and a conductor, evanescently confined in the perpendicular direction of their propagation. The number of applications that utilize SPPs has increased a lot during last decades including integrated optics and quantum optics as well. In our proposed on chip configuration with two arrays of meta-surfaces at the top of upper base, we demonstrated SPP based optical tractor beam while the exerted SPP becomes non-paraxial enough with the periodic array structure and base of the chip. Such beams can pull all objects within Mie-range in an on chip configuration facilitate other applications such as on chip manipulation and analysis of nanoparticles.

1.1 OPTICAL MANIPULATION

Optical manipulation makes use of the mechanical effect of light to exert force over the illuminated object. There are various types of optical manipulation techniques that are used in the field of science and medicine, and among these various types, optical pulling force has recently received a lot of popularity because it constitutes a rich family of counterintuitive phenomena compared with traditional manipulation techniques and also has profound physics underneath and has the prospect of being used in a large number of applications. The application of exerting is not just limited to the incidence of a plane polarized wave, rather other forms of waves such as acoustic, water and quantum matter waves can also be used or integrated. Furthermore, we can also include the progresses in the counterintuitive left-handed optical torque and lateral optical force as the extensions of pulling force, this phenomena can be used in application of remote mass transportation optical rotating and optical sorting.

In 1619, Kepler proposed the hypothesis that light carries momentum thus gives a radiation pressure on the illuminated objects. Later this hypothesis is proven right theoretically by Maxwell in classical electro-dynamic theory in 1873. Later in 1899, Russian physicist Lebedev experimentally demonstrated the light momentum carried by light on a solid body. This supports Maxwell's theory as well as Kepler's hypothesis. American physicists Nichols and Hull also demonstrated similar experiment at the same time and verified light momentum. From 1619 to 1903, within this progress, people realized the essence of light momentum.

Since light carries momentum, the interchange of momentum between light and object will generate a force, which is called optical force. Manipulations to objects by using this optical force is called optical manipulation. Optical manipulation is used now in various disciplines like biophysics, atomic physics, quantum science technology and nanotechnology. Up to now, two Nobel Prizes of physics have been awarded to the researches directly related to optical force and manipulation. The first was awarded to Steven Chu, Claude Cohen-Tannoudji and William D. Phillip in 1997 due to their work on the atom cooling using lasers and the second one was awarded to Arthur Ashkin in 2018 due to the invention of optical tweezers and promoting their applications in biophysics.

1.2 Optical Pulling force and tractor beam:

In our research, we demonstrated all object optical tractor beam using surface plasmon polariton. Our on-chip setup (which is coming in the next section) using a simple laser beam going in +Z direction and hits at the center of chip underneath and creates two SPP (surface plasmon polariton) in the upper plain (metal substrate). Amplitude and phase of SPP can be controlled using two arrays of rectangular nanostructures made of gold (Au).

Basically, we are using a counterintuitive phenomenon where all object (dielectric, plasmonic, chiral) is being pulled towards the source. In 2006, Marston at first predicted this in acoustics and very soon was extended to optics. The beam that can generate a pulling force is named a tractor beam. When an incident beam hits an object or particle, light matter interaction causing optical force and this force is controlled by three factors: the properties of the object, the light beam and the background medium. By tuning one, two or all three factors to some critical conditions, optical pulling force becomes possible. We can consider two simple examples to understand optical pulling force. First, when the object is made of an active medium with optical gain, more photons will be emitted than the incident ones due to the stimulated emission. Now, here in this case, backward pulling force is possible according to linear momentum conservation. Second, when we use a structured light beam superposed by a serials of plane waves, of which the momentums are off-axial with the average light energy propagation, a pulling force on the object is also possible when the elementary plane waves are directed to the average energy direction by an object. By these two examples we can understand the counterintuitive pulling force is compatible with the linear momentum conservation law. Light beams can be created in various structures of forms, which provide more choices for the pulling force generation.

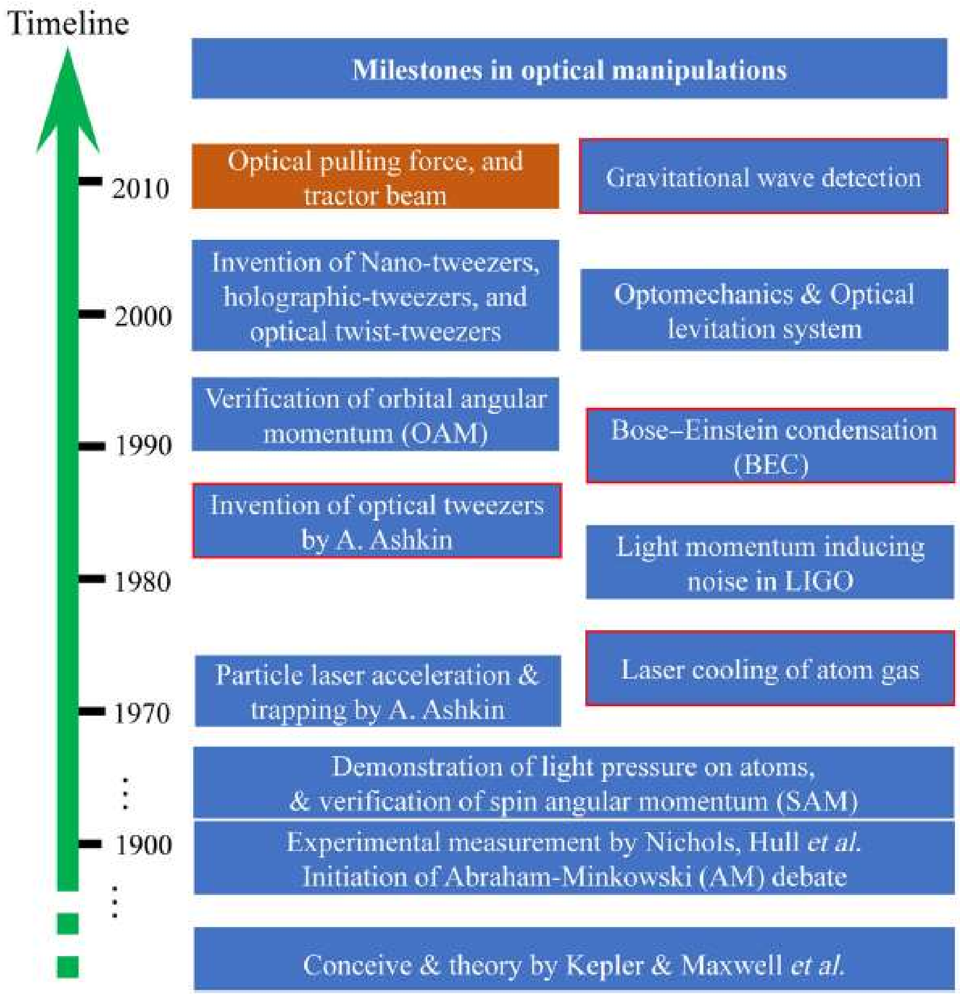

Figure1.1: A timeline illustration on the milestones in the development of optical forces and their application.

Chapter2: Setup and Method

In our research, we proposed and simulated a novel methodology for on chip configuration with meta-surface for generating non-paraxial surface wave, surface plasmon polariton which enables the possibility of pulling all objects (dielectric, plasmonic, chiral) within certain diameter range towards the source of light or radiation. Surface plasmon polariton (SPP) has received a great deal of attention due to its ability to direct light in the sub-wavelength scale. Here, one pair of SPP waves is generated on the gold film surface of the chip with the help of nanostructures when an incident laser beam is directed upwards underneath the chip. The two SPP waves propagating in X direction, decaying in z direction and forming an inference pattern in Y direction creates a source of SPP cosine beam. In our on chip set up we were being able to pull all object towards the source of radiation using SPP because by using gratings of nanostructures also known as meta-surface on the chip it becomes possible to control the amplitude and phase of surface wave in such a way that the exerted SPP waves becomes non paraxial enough to pull an object towards the source.

2.1: On-chip setup and generation of non-paraxial SPP

For our research work, all object optical tractor beam by surface plasmon polariton, we designed and simulated our setup in Comsol Multiphysics software and also verified our result with another software named Lumerical FDTD software.

We designed an on-chip configuration in Comsol Multiphysics, (Fig2.1). In our on-chip configuration, in the air medium, a plasmonic substrate of 100nm thickness is placed over a dielectric substrate of 200nm thickness. Both of these substrate layers are of 11.2μm and 3.2μm width which enables the generated field to have a propagation invariant region of about 2um length. A laser beam is propagating in +Z direction hits underneath the chip and creates surface wave surface plasmon polariton on the upper plasmonic substrate at the metal-dielectric interface of gold (Au-Johnson & Christy) and air medium. Generating optical pulling force using the exerted SPP waves becomes possible only when the waves becomes non-paraxial enough, then they could pull instead of pushing the illuminated object all the way towards the light source, i.e. optical tractor beams. Generation of tractor beam using SPP is possible, however there lies inefficiency if the wave propagates freely as the tractor beam comes into effect for objects with larger diameter. This is mitigated by making the beam non paraxial enough, by modulating the amplitude and phase profile of the incident beam. We placed two arrays of periodic grating structure of sub-wavelength dimensions, called metasurfaces, on the plasmonic substrate at the metal-dielectric interface in order to control both phase and amplitude of generated SPP waves so that they become non paraxial enough to pull the object towards the source of radiation. Placement of such arrays enable polarization dependent controlled and adjustable directional coupling through which facilitation of both bidirectional and unidirectional propagation of non paraxial SPP is possible.

A spherical particle is placed on chip (on plasmonic substrate) which is basically in the air medium. The vertical gap between the particle and the substrate is set to 30nm and the particle is placed 1.5μm away horizontally from mid-point of arrays. As in our on-chip setup, we can control the phase and amplitude profile of the generated SPP waves thus becomes non paraxial, we were able to pull all objects (in Comsol Multiphysics, we change the material and material property inside the spherical particle, we use dielectric, plasmonic and chiral material as spherical particle) towards the source of radiation. The proposed setup just requires a laser beam incident underneath the chip rather than aligning complex optical elements and this could be integrated to lab-on-a-chip platform and microfluidic devices for the analysis and sorting of biomolecules and nanoparticles.

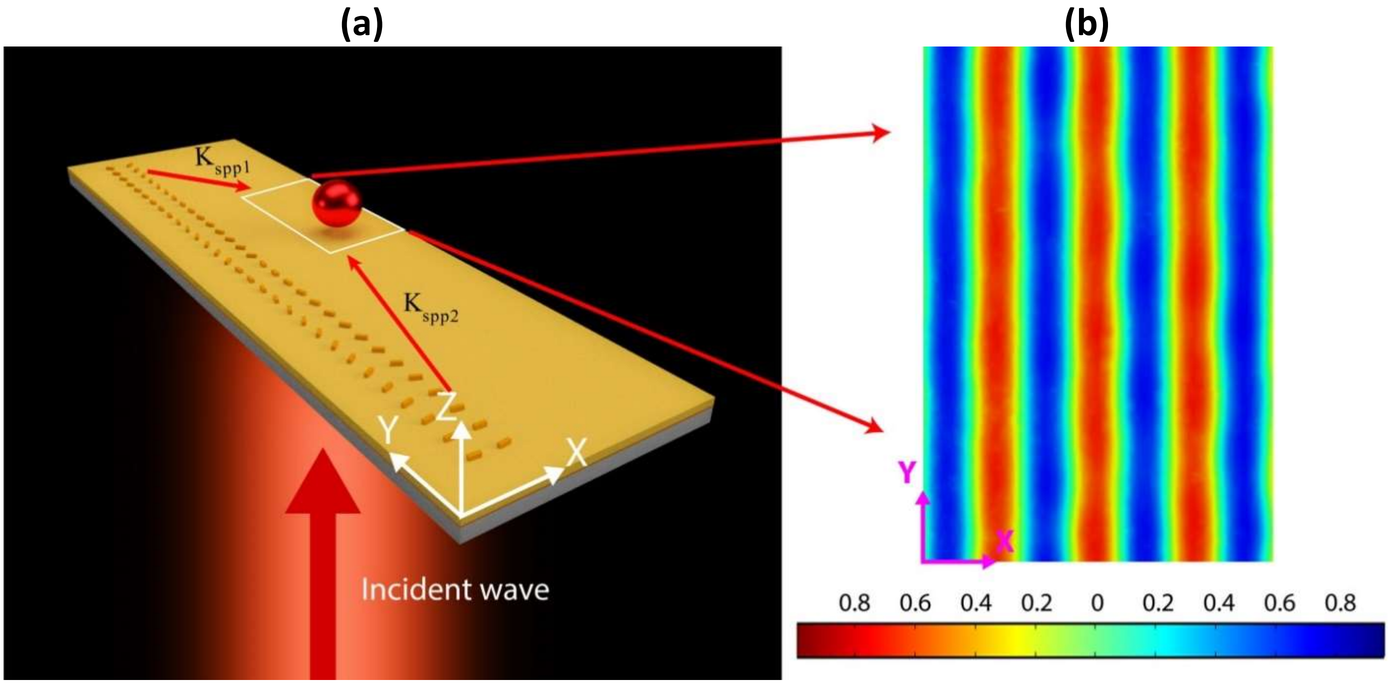

Figure 2.1: (a) A schematic of the proposed on-chip setup where the incidence of an x-polarized optical beam propagating in the +z direction leads to the conversion of a free propagating wave to an evanescently confined surface SPP wave. The arrows show a pair of SPP waves getting launched from the arrays and their superposition is creating an interference pattern. The vertical gap between the particle and the substrate is set to 30nm and the particle is placed 1.5$\boldsymbol{\mu m}$ away horizontally from the mid-point of the arrays. (b) A close up view of the interference field formed over the substrate where the central region has a continuous distribution of electric field.

2.2: Methodology and realizing SPP as tractor beam

A pair of nanoslit arrays made of gold (Au-Johnson & Christy) also known as meta-surface is used here in order to modulate the phase profile and amplitude profile of the SPP wave. Here, each array length is of about 5 μm and the generated field has a propagation invariant region of about 2 μm length. The spacing between the arrays has been set as $\lambda_{SPP}/2$ which enables the generation of a plane wave SPP field on the normal illumination of the incident field. Here, the benefit of our on-chip setup is that we just use an incident laser beam underneath the chip which hits the chip at the lower surface at the center of di-electric substrate and then it travels through the 200**nm** dielectric substrate and then 100**nm** plasmonic substrate and then creates surface waves surface plasmon polariton in short SPP wave at the metal di-electric interface of plasmonic substrate.

In order to, make the SPP waves non-paraxial we set the two arrays of meta-surfaces in a periodic fashion. Each array has 30 slits, total 60 slits in two arrays. Nano-slit angles are gradually increased from top to bottom across the array and they are tuned in such a way that the generated SPP waves becomes non-paraxial enough. Due to the arrangement of the two nano-slits, two waves get excited and launched with angle θ below and above the horizontal from the top and bottom region of the array where progressive increment of the meta-surface cell's tilt angle in the right array produces a constant wave vector $k_{SPP}\sin(\theta)$ in Y direction. Similarly, another wave gets launched from the lower array and the resulting non-paraxial beam gets formed in the central region of the substrate **(Fig. 2.1b)** due to the superposition of these two waves, that contributes to formation of the optical tractor beam. The angular difference between the two array is set to $\boldsymbol{\frac{\pi}{2}}$ to maintain a constant magnitude across the array **(Fig. 2.3)**. Non-paraxiality of the wave is validated as the superposition of these two local SPP wave leads to the formation of an optical tractor beam in the central region of the plasmonic substrate.

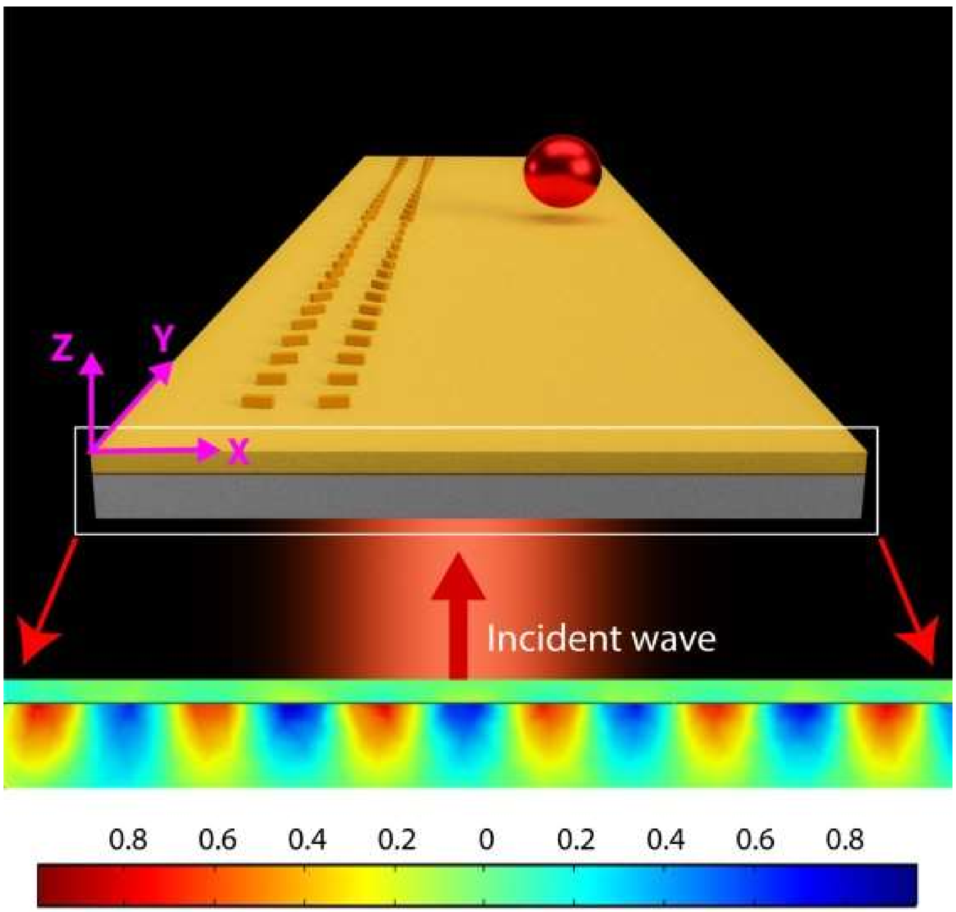

Figure.2.2 Presents a side view of the on-chip structure along with the field distribution of (E_z) formed across the substrate. Here, a plasmonic substrate of 100nm thickness is placed over a dielectric substrate of 200nm thickness. Both these layers are of 11.2μm length and 3.2μm width which enables the generated field to have a propagation invariant region of about 2μm length.

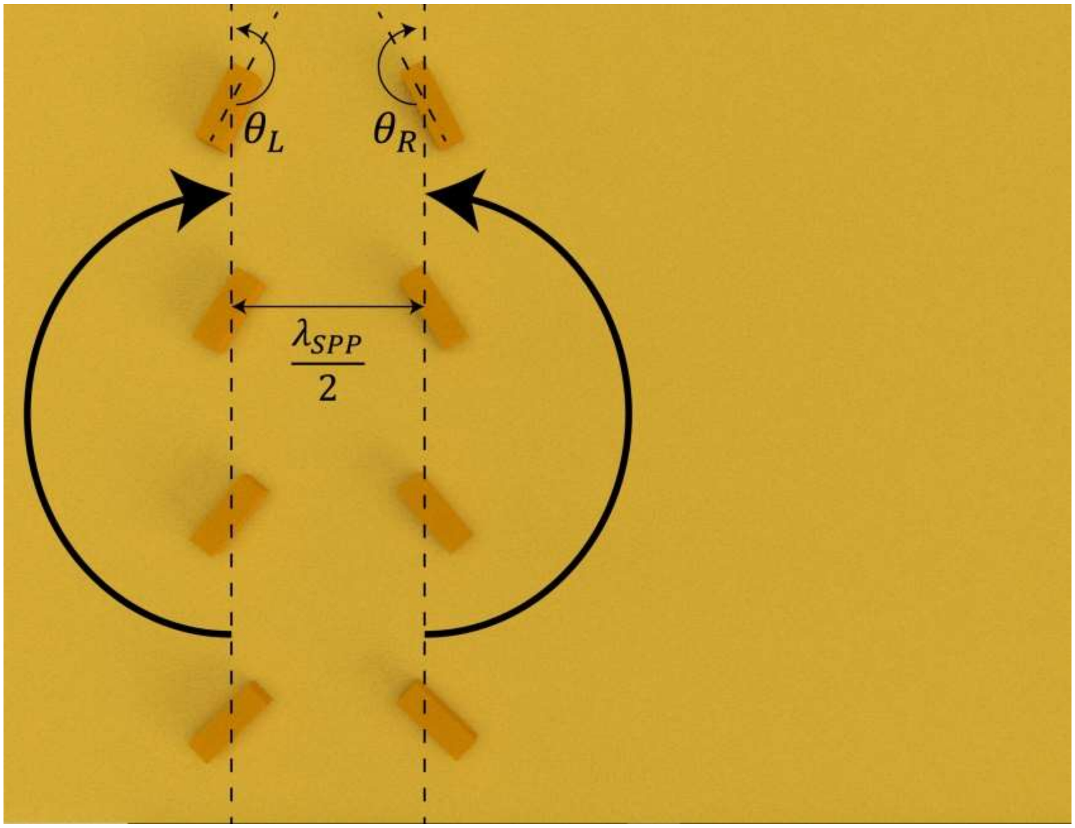

Figure 2.3: Here Nano-slit arrangement on chip configuration in a periodic fashion. Angles are gradually increased from top to bottom across the array in order to modulate the phase profile and amplitude profile of the exerted SPP waves. Each array has 30 slits, total 60 slits in two arrays. The angular difference between the two array is set to $\frac{\pi}{2}$ to maintain a constant magnitude across the array. The spacing between the arrays has been set as $\lambda_{SPP}/2$ which enables the generation of a plane wave SPP field on the normal illumination of the incident field.

Earlier work has been done where a single array has been used but we found that two arrays on the chip setup makes it possible to make non-paraxial beam where in case of single array only phase profile of generated SPP is controllable leaving the amplitude profile, so we use two arrays of meta-surface here. The designed on-chip configuration converts an x-polarized incident optical beam into an evanescently confined surface wave (SPP), where meta-surface nanostructures modulate the phase and amplitude profile of the SPP beam. The incidence of a x-polarized light, propagating in the +z direction comes into the contact with the dielectric substrate first and then travels along this to the plasmonic substrate, assuming that the incident light satisfies the first or second Kerker condition. This incident beam has a phase gradient $\boldsymbol{\xi_x}$ along the y direction, and the wave-vector components of the incident light are kx,i=0, ky,i=0, kz,i=k0, where k0 is the propagation constant in free space (equ 4). Now, following the law of conservation of momentum, the wave-vector components of the transmissive beam can be expressed as:

$$K_{x,t}=\boldsymbol{\xi_x},\ K_{y,t}=0,\ K_{z,t}=\sqrt{\boldsymbol{k_0^2-\xi_x}}$$

From the above equations we can see that when the phase gradient becomes larger that k_0 ($\boldsymbol{\xi_x}>k_0$), $K_{z,t}$ becomes imaginary, thus giving rise to an SPP wave propagating along the interface(Fig.2.2).

Here, surface waves are created in the vicinity of plasmonic substrate at the metal dielectric interface. Without the meta-surface or nanoslits, only at the presence of two substrate side by side in +Z direction and a spherical particle which is 30nm above the chip, these exerted SPP waves have properties for optical micro-manipulation, but for our purposes which is pull the object (spherical dielectric, plasmonic, chiral particle) to the source of radiation, the generated SPP waves should be non-paraxial enough. So, here comes the utility of two arrays of meta-surfaces which are set at the left side of the chip in order to modulate the phase profile and amplitude profile of the generated SPP waves in such a way that they become non-paraxial enough to pull the particle thus realize the SPP waves as tractor beams. electric field associated with the SPP wave's superposition in the central region can be written as:

$$\mathbf{E}_z = \mathrm{A}\exp(j\cos\theta\; k_{spp}\; x)\cos(\sin\theta\; k_{spp}\; y)\exp(-k_z z).$$

Where K_{SPP} represents the wave number of the SPP, which is as follows:

$$k_{spp} = k_0\sqrt{\frac{\varepsilon_m \varepsilon_d}{\varepsilon_m + \varepsilon_d}} \qquad k_z = k_0\sqrt{\frac{-\varepsilon_d^{\;2}}{\varepsilon_m + \varepsilon_d}}$$

Here, $\boldsymbol{\varepsilon_m}$ is relative permittivity of plasmonic material $\boldsymbol{\varepsilon_d}$ is relative permittivity of dielectric material, k_0 is the wave number in free space. The field propagates in the X direction while decaying in Z and forming a cosine pattern in y, thereby being referred to as a cosine SPP wave.

CHAPTER 3: Realizing Tractor Beam -Dielectric

Realizing optical pulling force on dielectric nanoparticles was one of the primary goals of our research work. For our simulation, the permittivity and refractive index was set such that the parameters were that of a Silicon Dioxide (SiO_2) material where the permittivity was (ε=3.9) and refractive index was set to 1.45, which is the real component of this value and as the material is a lossless material, the imaginary part of this value was set to 0. The background medium was set to that of air having a refractive index of 1. Looking at Fig:3.1 we can observe how the refractive index of SiO_2 varies with variation in the wavelength of the incident beam. The refractive index was chosen based on the wavelength of our incident beam ($\lambda = 632nm$).

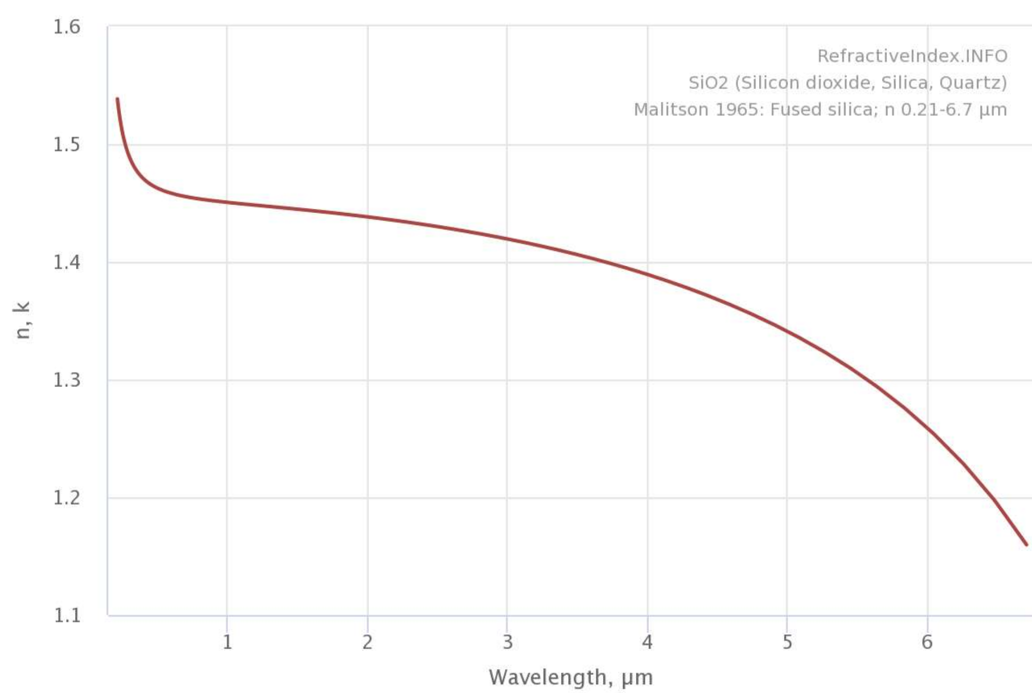

Fig 3.1: Variation of Refractive index of $\boldsymbol{SiO_2}$ with change in incident beam wavelength

We were able to realize optical pulling force being exerted over SiO_2 $(Dielectric)$ particles that were within the mie-range. The particles in the Rayleigh range always experienced a pushing force in the horizontal direction (positive (+)X axis) whereas the particles in the mie-range always experienced a pulling force in the horizontal direction (negative (-)X axis). Fig:2 shows how this pulling force exerted over the particle varied for particle diameter of 20nm – 250 nm. This result was obtained for a SiO_2 $(Dielectric)$ nanosphere placed at a horizontal distance of 1.5μm away from the array so that it was able to come in contact with the interference field formed by the superposition of the two SPP beams that were excited by the upper and lower portion of the metasurface arrays.

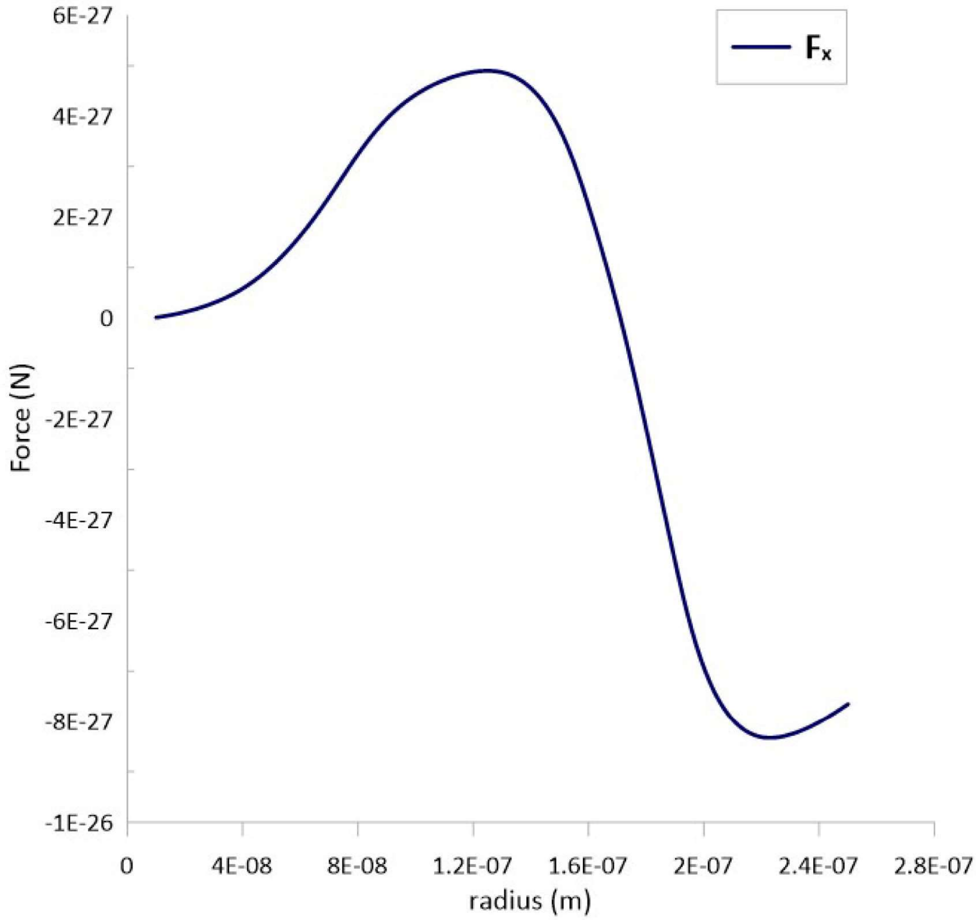

Fig 3.2: Optical force on SiO_2 (Dielectric) nanosphere with different radii (20nm – 250nm) when they are placed in the interference field. The negative 'X' force represents optical pulling force whereas the positive 'X' force represents pushing force.

The primary physics of this backward force that the SiO_2 (Dielectric) particle experiences is due to the induction of field excited multipole radiation that leads to multipolar expansion of electric and magnetic poles within the particle. As discussed earlier, this backward pulling force can only be realized when the interference field formed by the superposition of the two SPP beams becomes non-paraxial. Realizing this pulling force for certain radius range meant that the size of the impinged particle also played a role in achievement of this non-paraxial nature of the interference field.

For our numeric verification, we calculated the optical force on the illuminated SiO_2 (Dielectric) nanosphere to validate and explain its function as a tractor beam. We can express the time averaged optical force on the SiO_2 (Dielectric) particle that placed in the monochromatic field in terms of such said multipoles upto electric quadrupoles as:-

$$\boldsymbol{F} = \boldsymbol{F_{incident}} + \boldsymbol{F_{interference}}$$

Where $\boldsymbol{F_{incident}}$ actually contains the terms $F_p + F_m + F_{Qe}$+…. Here, subscript P refers to the force contribution due to electric dipole, m refers to the force contribution due to magnetic dipole and Qe refers to the force contribution due to electric quadrupole. The second term in the equation contains the terms $F_{pm} + F_{Qep}$ +…… Here, subscript PM refers to the force contribution due to the interaction of electric and magnetic dipoles and subscript Qep refers to the force contribution due to electric quadrupoles. These two terms can be further expanded to explain relation with the induced electric and magnetic field. The three terms in $F_{incident}$ can be expanded as:-

$$(\boldsymbol{F_{incident}})_x = \frac{1}{2}\,\mathrm{Re}[(\nabla \boldsymbol{E}^*).\mathrm{p}] + \frac{1}{2}\,\mathrm{Re}[(\nabla \boldsymbol{B}^*).\mathrm{m} + \frac{1}{4}\,\mathrm{Re}[(\nabla\nabla \boldsymbol{E}^*).\mathrm{Q_e}$$

Whereas the two terms in $\mathbf{F_{interference}}$ can be expanded as:-

$$(\boldsymbol{F_{interference}})_x = -\frac{\boldsymbol{k^4}}{\boldsymbol{12\pi\varepsilon_0 c}}\mathrm{Re}[\mathrm{pxm}^*] - \frac{\boldsymbol{k^5}}{\boldsymbol{40\pi\varepsilon_0}}\mathrm{Re}\,[\mathrm{Q_e.p}^*]$$

Where E & H are incident electric and magnetic field and p and Q_e are electric dipole and quadrupole moment & m is the magnetic dipole moment where p=α_eE & m=$\alpha_m H$. Q_e=$\left(\frac{\gamma_e}{2}\right)(\nabla E+\nabla E^T)$, $a_e=\frac{i6\pi\varepsilon_0 a_1}{k^3}$,$a_m=\frac{i6\pi b_1}{k^3\mu_0}$ and $\gamma_e=\frac{i40\pi\varepsilon_0 a_2}{k^5}$ are complex polarizabilities, a_1, a_2, a_3 are the Mie coefficients and k is the wave vector.

We observe that the negative force arises when $F_{interference}$ is greater than $F_{incident-}$. Every term in $F_{interference-x}$ is the product of two multipoles which represents the backward force induced by the interference field expressed above.

As discussed above, the mathematical interpretation of this backward pulling force can be directly correlated with the presence of such dipoles and quadrupoles. Now, looking at Fig:3.3 we will be able to see the physical plot of these said poles.

(a)

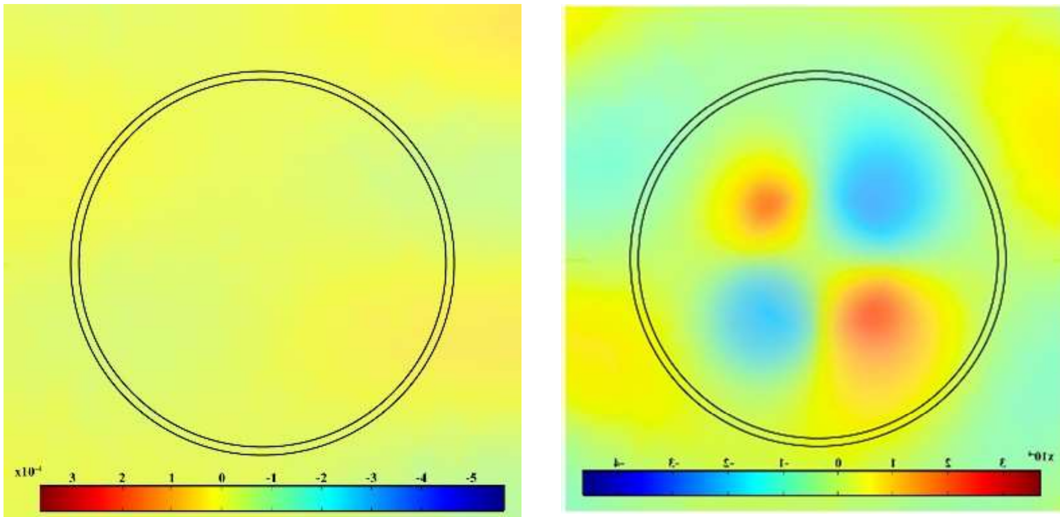

(b)

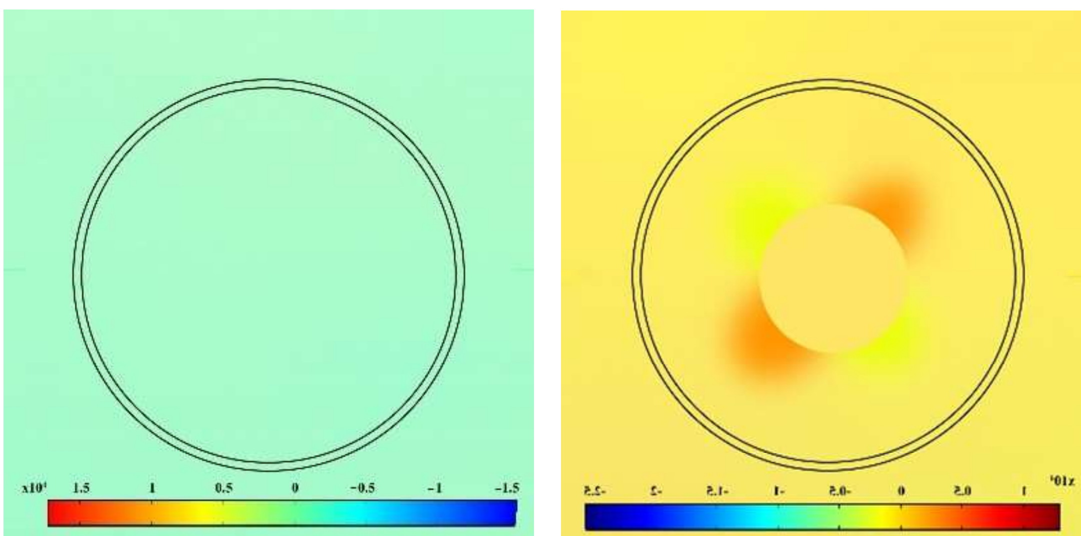

Figure. 3.3 (a)- (b) Shows the Magnetic Field and Current Density respectively in the SiO_2 (Dielectric) particle for 70nm and 190nm where the particle experiences a pushing force for the former and a pulling force for the latter. No apparent pole formation can be seen for the pushing case whereas emergence of quadrupoles are visible for the pulling case which shows field excited multipole radiation is occurring in the particle when tractor beam comes into effect.

From the figure 3.3 we can see that the radius range within which the particle experienced a pushing force was due to the fact that no significant pole formation occurred within the particle which gives rise to the pulling force. So, we can say that within this range, the system is behaving very much intuitively where the direction of force exerted over the particle will be similar to the propagation direction as per the conservation law of momentum, whereas, in case of the diameter where apparent pulling force has been observed in the particle, electric and magnetic poles have emerged. Emergence of such poles and their moment has enabled us to obtain a nonconservative pulling force for SiO_2 (Dielectric) nanospheres.

CHAPTER 4: Realizing Tractor Beam – Plasmonic

Realizing optical pulling force on plasmonic nanoparticles was the second goal of our research work as our primary goal was to design and implement a setup where all-object tractor beam can be acquired. For our simulation, the refractive index of the said particle was set such that it resembled that of Gold (Au Johnson and Christy 1972). Since gold is a lossy material, the refractive index was a complex one where for an incident beam of ($\lambda = 632nm$) the complex refractive index was found to be (0.19+3.42i) where 0.19 is the real part of the refractive index and 3.42 is the complex or imaginary part, resembling the lossy component of this material. Fig:1 below shows how the real and complex component of this value varies with change in incident beam wavelength. And similar to all our previous setups, the background medium was considered to be that of air where the refractive index is set to 1(Real Component).

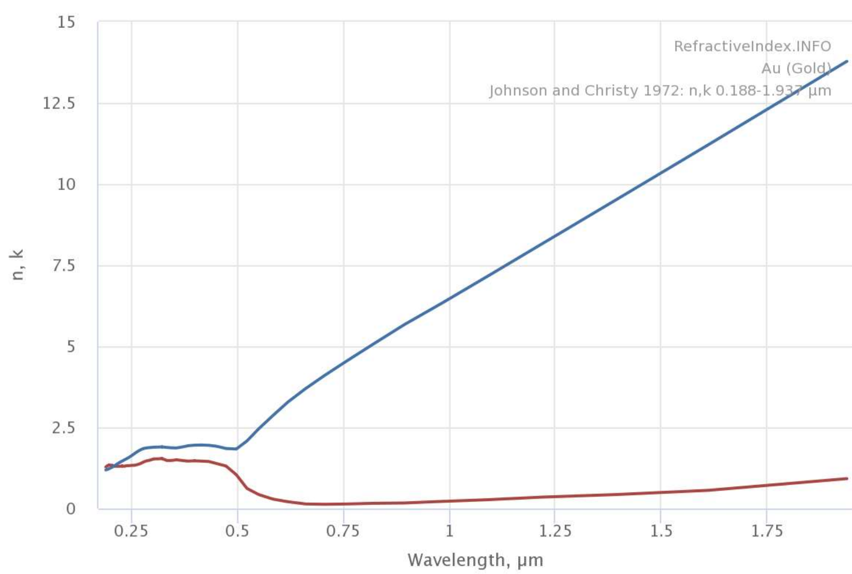

Fig 4.1: Variation of Refractive index of $\boldsymbol{Au(Johnson\ \&\ Christy)}$ with change in incident beam wavelength. Here the blue line indicates the variation in real

component of the refractive index and the brown line indicates the complex part.

Similar methods of simulation was followed and we were able to obtain or realize optical pulling force for plasmonic nanospheres within the radius range of 20nm – 150nm which is also known as the mie range whereas in the radius range of 160 nm Rayleigh range, pushing force was observed. Fig:4.2 below shows how this force varied with change in diameter of the plasmonic nanoparticle. This pushing and pulling was observed in the horizontal direction where pushing force meant the particle will experience force that will be pointed towards the positive X direction and a pulling force indicates a force acting towards the negative X direction. Similar to our earlier setup, the nanoparticle was placed at a distance of 1.5μm away from the midpoint of our arrays such that the interference field formed by the superposition of the two SPP beams launched from the upper and lower region of our metasurface arrays impinged upon the particle. This placement is crucial for our work as the whole work is based on obtaining optical tractor beam by the superposition of the complex wave which can establish a tractor beam when it becomes non paraxial.

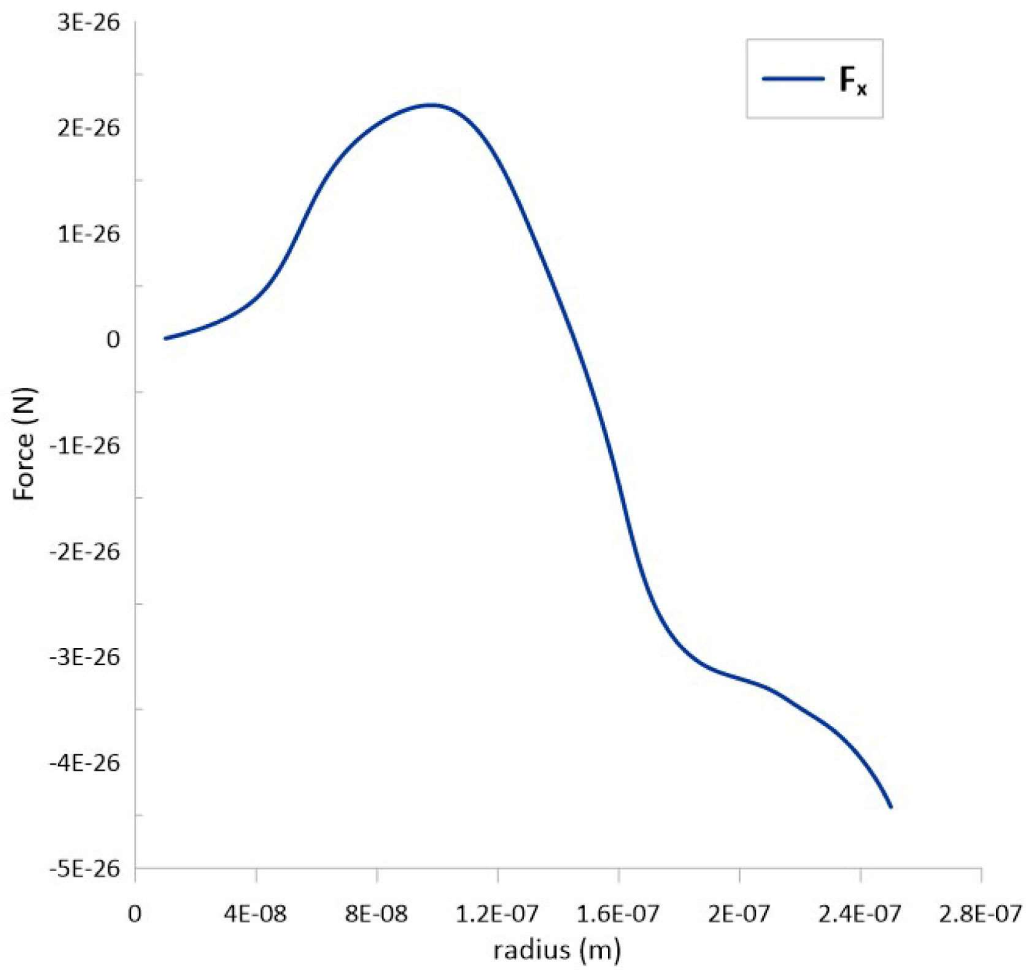

Fig 4.2: Optical force on Au(Johnson & Christy) or Plasmonic nanosphere with different radii (20nm – 250nm) when they are placed in the interference field. The particle experiences pushing force upto a radius of 150nm and pulling force is being realized from 160nm onwards. The negative 'X' force represents optical pulling force whereas the positive 'X' force represents pushing,

The primary physics of this backward force that the Plasmonic particle experiences is due to the reversal of electric field along with a distribution of magnetic field over the plasmonic substrate. This reversal of electric field **(Fig: 4.3)** causes the bounce charge and current within the plasmonic nanosphere to experience a force that occurs in the negative x direction thus giving rise to pulling force. To mathematically explain this phenomena, we followed a different approach where Lorentz Force equation was used to reveal how this pulling force is originating in the system, whereas the mathematical iterations done in our simulation was using time averaged MST (Maxwell's Stress Tensor) technique. Both the approaches, however, has allowed us to come to a conclusion that our numerical results were indeed supporting or validating the experimental results obtained from our simulations as both showed the same nature of pulling and pushing force.

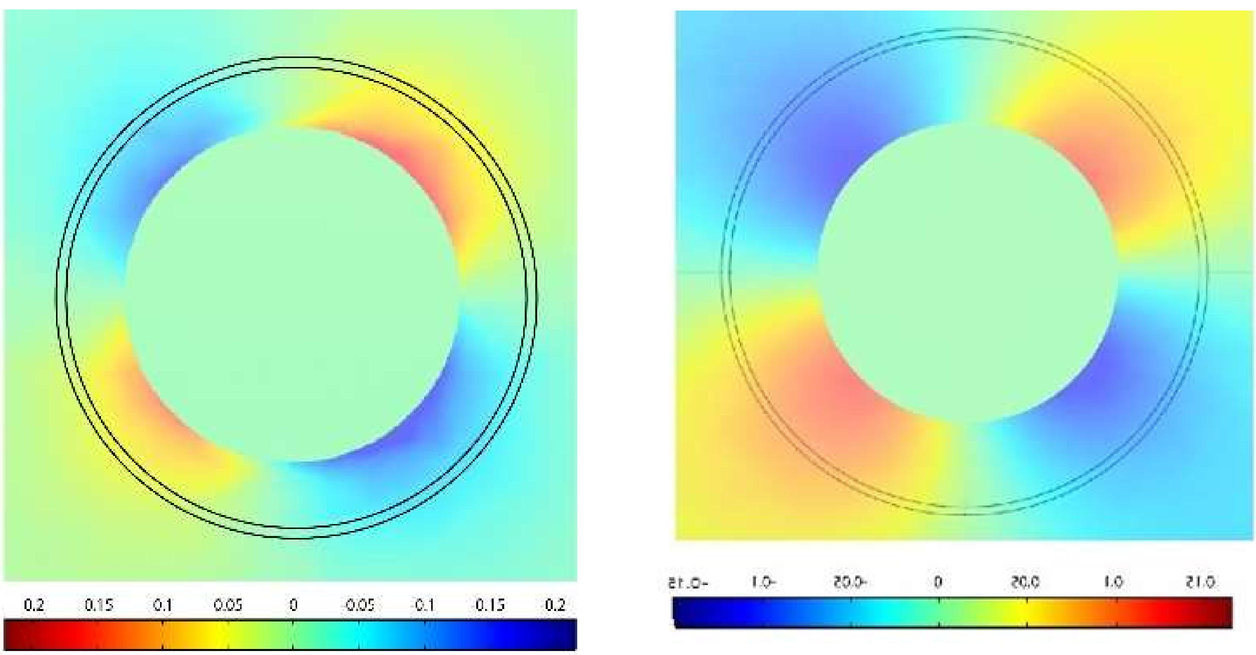

Fig 4.3:Shows Electric Field distribution in the plasmonic particle for a radius of 20nm when the particle experiences a pushing force and for 190nm when the particle experiences a pulling force. Reversal of field is induced by the interference field created by the SPP wave which contributes to the pulling force of the particle.

Using the Lorentz Force equation, we were able to realize the force contributions of the bound current (F_b) and the force contributions of the bound charge (F_c). In this part of our work, as we are working with plasmonic material which is nonmagnetic in nature, we considered the bound current density from the magnetization $\nabla \times M$ and the magnetic charge density $-\nabla . M$ to be zero. Hence, we can write the two parts of the Lorentz force density f_b and f_c as below:-

$$\boldsymbol{f_b = \frac{1}{2} Re[\varepsilon_0 (\nabla . E) E^* \text{-} i\omega \varepsilon_0 (\varepsilon_R - 1) ExB^*}$$

$$\boldsymbol{f_c = \frac{1}{2} Re[\omega \varepsilon_1 ExB^*]}$$

In the equation above**,** $\boldsymbol{\varepsilon_R}$ represents the real part of the particle's relative permittivity and $\boldsymbol{\varepsilon_1}$ represents the imaginary part. The first two terms in $\mathbf{f_b}$ represents the force on bound electric charge and current respectively whereas $\mathbf{f_c}$ represents the force contribution due to the free current. The net force exerted on the plasmonic particle is found by integrating the sum of $\mathbf{f_b}$ and $\mathbf{f_c}$ over the sphere.

The negative force comes into effect due to $\mathbf{f_c}$ becoming negative, which is induced by the interference field created by the superposition of the two SPP beams which produces extra momentum to the free current. This causes $\mathbf{f_c}$ to become dominating, and the pulling force gets enabled when $\mathbf{f_c}$ becomes greater than $\mathbf{f_b}$, which is further accompanied by the magnetic field distribution over the substrate (Fig: 4.4), which exerts this pulling force on the charge and current, dragging the plasmonic particle towards the meta-surface array. The reversal of electric quadrupole is in fact occurring as the magnitude and direction of energy flow is altering the force density on the induced current, causing the reversal of the direction of total force, as the field reversal leads to the reversal of $\mathbf{f_b}$ as well. We can clearly observe that the negative force is being realized due to the Lorentz Force on bound charge and current inside the particle.

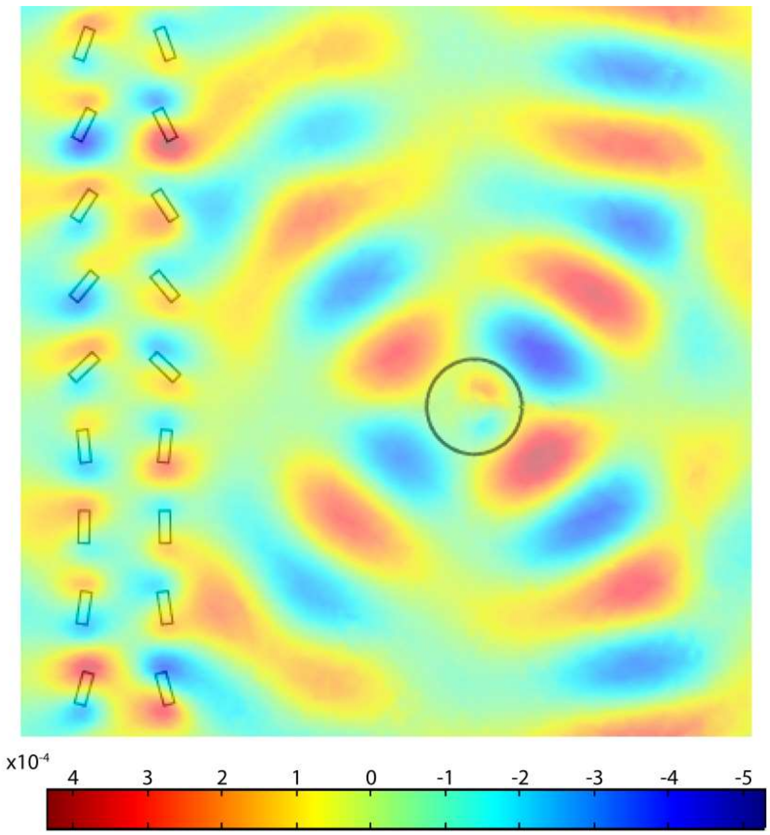

Fig:4.4 Distribution of Magnetic Field over the substrate of the on chip structure. The black circle indicated the position of the nanoparticle.

Unlike our findings in dielectric material where the field distribution within the dielectric particle was negligible for pushing case, which meant that the pushing force emerged due to the conservation of momentum, multipolar excitation occurred in plasmonic nanosphere from the very beginning (20 nm radius) which meant that the beam impinging on the particle leading to momentum conservation is not the only reason of this pushing force. This pushing force can also be explained using the Lorentz force equation. Here, f_c is actually a negative force that acts as the contributor. This is due to the fact that the force density on free currents in the plasmonic material is exerting a pushing force as the incident beam attenuates and transfers momentum to the free currents in this lossy material, that is, the plasmonic material.

CHAPTER 5: Realizing Tractor Beam - Chiral

As we have seen earlier non-paraxial SPP waves can pull both dielectric and plasmonic spherical particle within certain diameter range (Mie-range) applied on chip configuration, we observed optical pulling forces for chiral particle for 140nm and onwards in our on chip configuration as well in our Comsol simulation. Then we have done the same set up simulation for chiral particle in Lumerical software and observed the optical pulling force for 140**nm** and onwards for chiral particle, almost similar pulling force is found like Comsol. The design consisted of a plasmonic substrate at the top having a thickness of 100×10^{-9} m, which was placed over a dielectric substrate at the bottom having a thickness of 200×10^{-9} m and two arrays of meta-surfaces, each array having 30 nano-slits having dimensions of 47nm*140nm and the height of each nanoslit is 47nm, placed over the plasmonic substrate. Both substrates were placed in the air medium, and had widths of 11.2×10^{-6} m and 3.2×10^{-6} m respectively. A spherical chiral nanoparticle is placed slightly above the plasmonic substrate, with the vertical gap between the particle and the substrate being 30×10^{-9} m and the horizontal distance between the particle and the midpoint of the metasurface arrays was set at 1.5×10^{-6} m (figure-1). Thus we can realize non paraxial SPP waves as tractor beam for chiral particle as well. Then, using other useful techniques and features of Comsol Multiphysics, we investigate the whole set up and specially the chiral particle which is in the vicinity of the plasmonic substrate, for finding the light matter interaction which is contributing the counterintuitive phenomenon, this optical pulling force towards the source of radiation and we observed optical pulling force is acting on the chiral nanoparticle for 140nm radius and onwards, showing similar kind of optical pulling force acting on chiral nanoparticle as well.

5.1: Properties of chiral particle

A chiral is an object that is not identically superimposable with a mirror image of itself. An achiral is an object that is identically superimposable with a mirror image of itself. Here, we are using isotropic chiral particle in our set up. Incident field on chiral particle induces polarization currents on the particle which in the dipole approximation limit (for small particle) is denoted by electric and magnetic dipole moments p and m. Therefore, the constitutive relation between the induced electric and magnetic dipole moments and the incident electric E_{i} and magnetic E_{i} fields read:

$$\boldsymbol{p} = \boldsymbol{\alpha}_{\boldsymbol{ee}}\boldsymbol{E}_{\mathbf{i}} + \boldsymbol{\alpha}_{\boldsymbol{em}}\boldsymbol{H}_{\mathbf{i}};$$

$$\boldsymbol{m} = \boldsymbol{\alpha}_{\boldsymbol{me}}\boldsymbol{E}_{\mathbf{i}} + \boldsymbol{\alpha}_{\boldsymbol{mm}}\boldsymbol{E}_{\mathbf{i}}$$

Here, α_{ee}, α_{em}, α_{me} and α_{mm} are called polarizability of the particle: electric, magnetoelectric, electromagnetic, and magnetic ones, respectively. The polarizabilities linearly relate the incident electric and magnetic fields to the induced electric and magnetic dipole moments.

5.2: Optical pulling forces for chiral particle on chip configuration:

The optical force acting on a chiral particle is qualitatively different from that acting on achiral particle due to chirality dependent forces. For chiral particle, chirality-induced coupling can serve as a mechanism to realize optical pulling forces. The majority of research in optical micromanipulation focuses on the interaction of light with isotropic spherical particles. Simple spherical particles can be used as prototypes for an intuitive understanding of light matter interaction. But in case of chiral particle, realizing this light matter interaction is not so simple. Here, we have to take in consideration about chirality dependent optical forces acting on the chiral particle.

Here, in our on chip set up, a spherical chiral particle placed in the vicinity of the plasmonic substrate of the chip configuration and we are experiencing that a pulling force on the chiral particle is acting within the range of 140nm to 250nm of the chiral particle as shown in Fig: 5.1. Chirality property appearing in natural substance is usually weak, so we use artificial nanostructure or nano-sphere of chiral spherical particle to uplift chirality in our on chip set up. Chirality dependent forces that couple the mechanical linear momentum of photons with the angular momentum of photons will emerge, giving rise to counterintuitive phenomena such as optical pulling forces owning to the chirality of the particles.

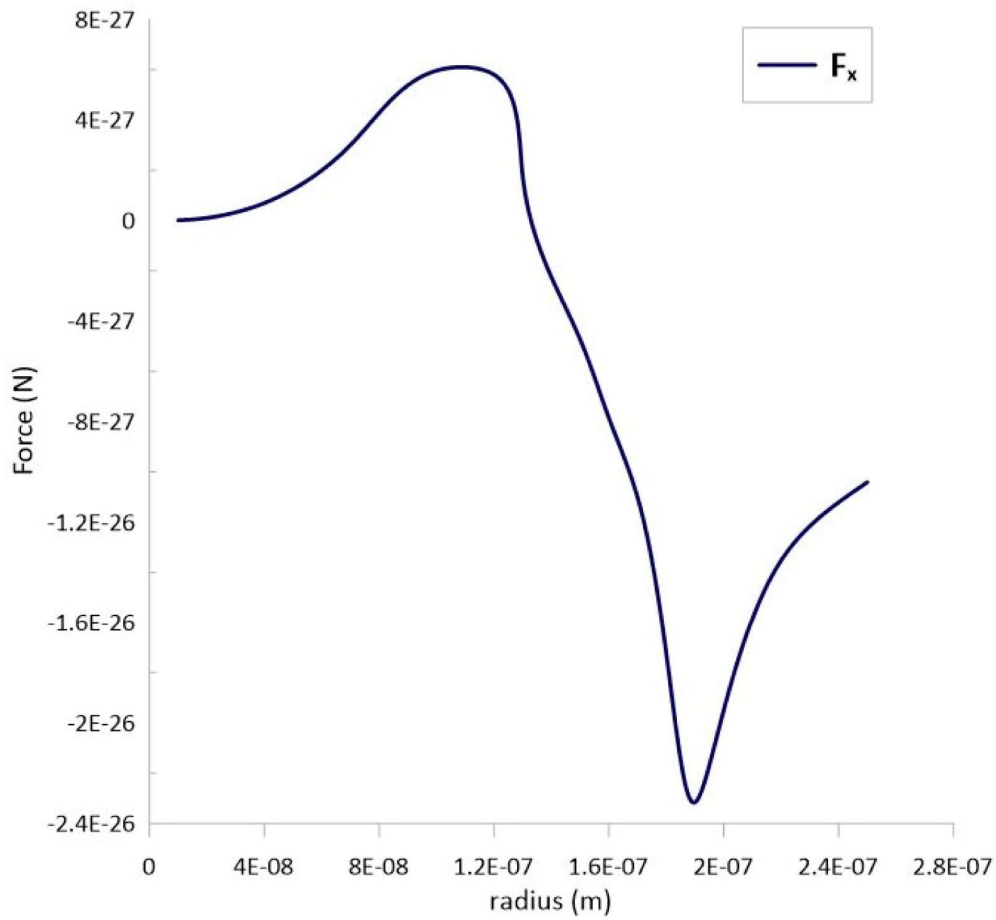

Fig: 5.1 Optical force on Chiral nanosphere with different radii (20nm – 250nm) when they are placed in the interference field. The particle experiences pushing force upto a radius of 130nm and pulling force is being realized from 140nm onwards. The negative ‘X’ force represents optical pulling force whereas the positive ‘X’ force represents pushing,

The chirality of a particle is manifested only when the particle interacts with another chiral entity. Electromagnetic waves can have a chiral character and as our excited SPP beams are monochromatic electromagnetic waves, they also exhibits chiral character and their time-averaged chirality flux can be defined as:

$$\langle \boldsymbol{\psi} \rangle = \langle \boldsymbol{\psi_e} \rangle + \langle \boldsymbol{\psi_m} \rangle$$

Where

$$\langle \boldsymbol{\psi_e} \rangle = \frac{\boldsymbol{\mu_0 \omega}}{\mathbf{4}} \boldsymbol{Im}\{\boldsymbol{\varepsilon_0 E^*} \times \boldsymbol{E}\}$$

$$\langle \boldsymbol{\psi_m} \rangle = \frac{\boldsymbol{\mu_0 \omega}}{\mathbf{4}} \boldsymbol{Im}\{\boldsymbol{\mu_0 H^*} \times \boldsymbol{H}\}$$

$\langle \boldsymbol{\psi_e} \rangle$ and $\langle \boldsymbol{\psi_m} \rangle$ are the portions of the chirality flux associated with the electric and magnetic fields respectively. In our on chip set up, a spherical chiral particle is placed in the vicinity of the upper plasmonic substrate which experiences an optical pulling force for particle within the radius range of 140nm to 250nm. Chirality property appearing in natural substance is usually weak, so in our on chip set up in Comsol Multiphysics we set the particle in the vicinity of the chip and chooses chiral material and gives it proper chirality related equations using features of Comsol Multiphysics, so we basically used artificial nanostructure of chiral spherical particle to uplift chirality in our on chip setup.

A nanostructured chiral spherical particle can be distinguished by an induced electric dipole moment **p** and magnetic dipole moment **m** where

$$\mathbf{p} = \vec{\alpha}^{ee}\mathbf{E} + \vec{\alpha}^{em}\mathbf{B}$$
$$\mathbf{m} = -\vec{\alpha}^{emT}\mathbf{E} + \vec{\alpha}^{mm}\mathbf{B}$$

Here superscript T denotes transpose, $\underset{\boldsymbol{a}}{\leftrightarrow}^{\boldsymbol{ee}}$, $\underset{\boldsymbol{a}}{\leftrightarrow}^{\boldsymbol{mm}}$ and $\underset{\boldsymbol{a}}{\leftrightarrow}^{\boldsymbol{em}}$ are respectively the electric, magnetic and chiral polarization tensors of the chiral particle. In case of chiral particle, $\underset{a}{\leftrightarrow}^{em}$ is a non zero term due to chirality of the constituting molecules or the chiral shape of the particle. A particle exhibits it's chirality when it interacts with another chiral entity.

It is clear that all terms that depend on $\underset{a}{\leftrightarrow}^{em}$ are related to the chirality of the particle. The designed on-chip structure converts an x-polarized incident optical beam into an evanescently confined surface wave (SPP), where the meta-surface nanostructures modulate the phase and amplitude profile of the SPP beam. The incidence of an x-polarized light, propagating in the +z direction comes into contact with the dielectric substrate and travels along this to the plasmonic substrate. As our generated SPP waves are monochromatic electromagnetic waves, they also exhibits chiral character and we know that the chirality of a particle is manifested only when the particle interacts with another chiral entity.

We put the chiral particle in our on chip set up in the vicinity of the chip in our simulation in Comsol Multiphysics and after completing our simulation, we find the optical pulling force (**Fx)** graph which is acting on the chiral particle, the particle experiences a pulling force towards the source of radiation within the radius range of 140nm to 250nm. We simulate the similar set up in Lumerical software and observed that the chiral particle is experiencing same pulling force acting on it.

We have find the potential of the chirality-dependent forces to pull a chiral particle towards the source of light. Now we have to analyze time averaged optical force exerted on the chiral particle. In our on chip set up, time average optical force on chiral particle in monochromatic optical field can be calculated by the following equation. Now, the multipole expansion of time averaged optical force exerted on the chiral particle impinged by the interference field created by the superposition of the two SPP beam propagating in x direction can be written as

$$\langle \boldsymbol{F} \rangle = \boldsymbol{F_p} + \boldsymbol{F_m} + \boldsymbol{F_{pXm}}$$

Where

$$\boldsymbol{F_p} = \frac{1}{2} \boldsymbol{Re}\{(\boldsymbol{\nabla E^*}).\mathrm{p}\}$$

$$\boldsymbol{F_m} = \frac{1}{2} \boldsymbol{Re}\{(\boldsymbol{\nabla B^*}).\mathrm{m}\}$$

$$\boldsymbol{F_{pXm}} = -\frac{\boldsymbol{k^4}}{\boldsymbol{12\pi\varepsilon_0 c}} Re\{\boldsymbol{pXm}\ ^*\}$$

The terms that depend on $\underset{\boldsymbol{a}}{\leftrightarrow}^{\boldsymbol{em}}$ are associated to the chirality of the particle. The optical force acting on a chiral particle is qualitatively different from that acting on an achiral particle due to the chirality dependent forces which couple mechanical linear momentum with optical spin angular momentum.

Here, the optical pulling force can be recognized by excitation of electric dipole **(Fig. 5.2)** moment **p** and magnetic dipole moment **m**. For chiral particle, a different approach for realizing optical pulling force is used that couples linear momentum with angular momentum via chirality.

The terms in force equation that contains the parameters contributing to the optical force are proportional to $\boldsymbol{\psi_e}$ and $\boldsymbol{\psi_m}$. These forces can be recognized as the chirality forces as they created from chirality fluxes of the field and the chirality of the particle $\underset{\boldsymbol{a}}{\leftrightarrow}^{\boldsymbol{em}}$**.** When the chirality dependent force terms in optical force equation are greater than the summation of the interaction force terms, an optical pulling force is acting on the chiral particle.

For the optical pulling force in equation, we use Maxwell stress tensor and multiple scattering theory to display that forces excited by chirality flux can create an optical pulling force on a chiral particle that is not optically small.

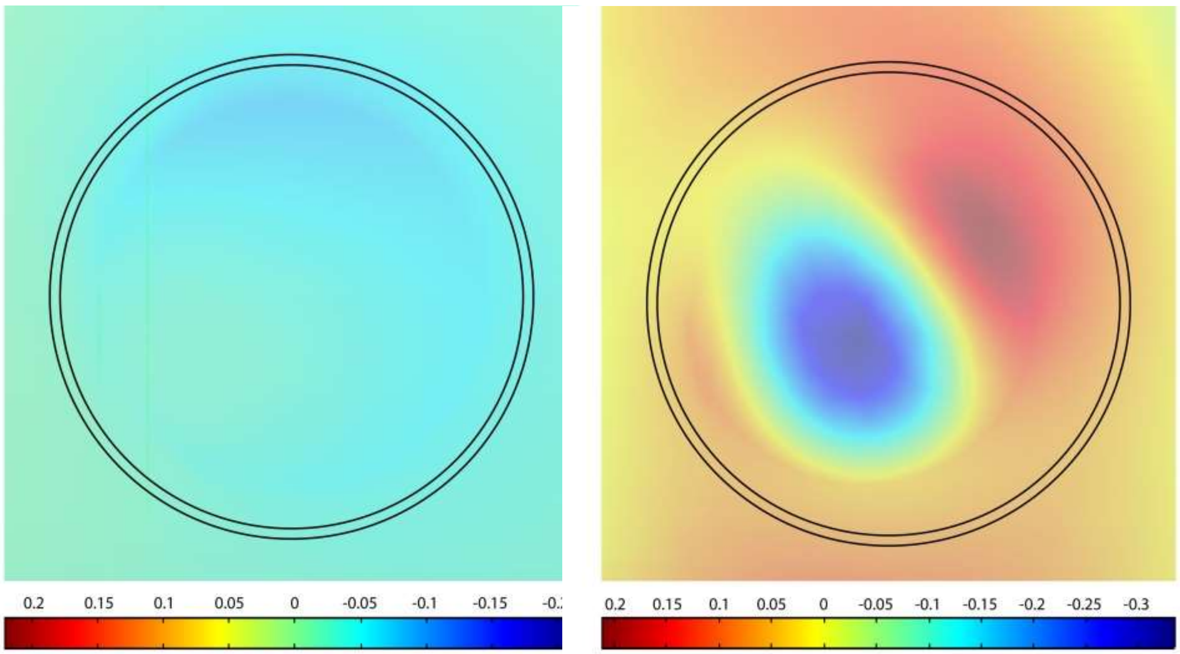

Figure. 5.2 Shows Electric Field distribution in the chiral particle for a radius of 70nm when the particle experiences a pushing force and for 160nm when the particle experiences a pulling force. No poles are observable for the pushing case whereas the emergence of field excited electric dipole is present for the latter, that contributes the optical pulling force experienced by the particle.

CHAPTER 6: CONCLUSION

In our research, all object optical tractor beam by surface plasmon polariton, we are being able to pull all objects (dielectric, plasmonic, chiral) by generating non-paraxial SPP beams using two arrays of metasurface on the chip configuration consisting of plasmonic and dielectric base. It shows new possible applications of surface waves as tractor beams and using this property SPPs can be used for sorting and analyzing of nanoparticles and biomolecules.

Surface plasmon polaritons (SPPs) have showed high potential for various applications in various fields, ranging from physics, chemistry, biology and integrated photonic circuits due to their the strong confinement of light to the metal surface. The number of applications that utilize SPPs has increased tremendously during the last decades, including energy harvesting, coupler or modulator in integrated optics, biosensing, sub-diffraction imaging and quantum optics. The great interest in SPPs results from their unique abilities such as the strong confinement of the field to the interface and their unique dispersion relation. However, the mismatch of the SPP momentum to that of free space photons prevents light from free space to couple efficiently into a SPP mode, making it necessary to add periodic structures or to modify the dispersion relation at the interfaces to satisfy momentum conservation. Several different approaches have been developed to excite SPPs for various application. More classical techniques like the Kretschmann or the Otto configuration use bulky prisms to alter the momentum of the incoming light beam through dispersion. These techniques are cumbersome to implement and impractical for flat optics technology and optical circuits with vertical integration. Previous studies so far have not demonstrated the full control of both excitation amplitude and phase of SPPs independently and simultaneously which is a crucial feature for launching light into integrated optical circuits. We used two arrays of metasurfaces to control the amplitude and phase of exerted SPPs of our on chip configuration. Metasurfaces are thin, scalable and capable of being easily integrated. Here, we present a novel approach for SPP excitation based on scalable ultrathin plasmonic metasurface which is able to provide a fully variable and independent control of phase and amplitude of excited SPPs. For our demonstration of amplitude and phase controlled SPP excitation we utilize two arrays of metasurfaces. Combining both effects such as metasurfaces based on nanoantenna structures are able to simultaneously tailor both the intensity and phase of SPPs. We arranged the metasurfaces or nano-slits in a periodic pattern with a constant gradient. To efficiently couple the incoming free space light into a SPP wave, it is important to keep the distance between the nano-slits and plasmonic gold substrate as small as possible because of the evanescently confined nature of SPP.

When optical tweezers – which allow for holding and moving microscopic objects such as droplets, atoms and nanoparticles with the help of a highly focused laser beam – were discovered in the 1970s, scientists were introduced to a whole new field of research, where they could manipulate different parameters of an incident light beam to exert non-conservative forces on the illuminated object. With further advancements in research, scientists were able to transform the optical tweezer in to a powerful tool with crucial manipulative properties on micro and nanoparticles in various scientific fields. With the help of the increased and improved usability of the optical tweezer, scientists could now tap in to the potential of sorting, trapping and binding of particles on a micro and nanoscale. This opened further pathways in scientific research, with applications across a diverse range of fields in biology, biomedicine, microfluidics – which refer to the behavior, control and manipulation of fluids by micro components in the fields of engineering, physics, chemistry, biochemistry, biotechnology and nanotechnology – and colloidal science, where minuscule particles are evenly distributed in a mixture of two or more substances. Study and research on optical pulling forces is also an integral part in disciplines such as biophysics, atom physics and quantum science technology. The application of exerting pulling forces is not limited to only beams of plane polarized light, but also reaches out to other wave forms including acoustic, water and quantum matter waves.

6.1 Future Works

As we delve further in to the Information Age, where accessibility and usability of data and information is progressing faster than at any time in the past, mankind is being equipped with increasingly powerful tools to study and research using all the data and information, which has made the possibilities greater than ever before. In this flow, research on optics can lead to newer and greater discoveries, and the work demonstrated in this paper can provide the base for further research in the future to realize achievements on a variety of topics, such as the analysis of biomolecules by the sorting of particles in an inhomogeneous mixture. Our work can also assist in levitation dynamics in optomechanical systems, and active and passive feedback schemes for realizing quantum mechanical superposition – one of the fundamental principles of quantum mechanics which states that much like waves, any two quantum states can be added together and the result will be a superposed and valid quantum state, represented as the sum of the other distinct quantum states. Moreover, ground state cooling can be researched and realized based on the findings of our work, as well as the coherent manipulation of mechanical systems – which is a method based on quantum mechanics which allow for controlling quantum interference phenomena by shaping the phase of laser light pulses. Furthermore, because research on optical pulling force constitutes counterintuitive phenomena compared to traditional manipulative techniques, the strong physics underlying optical pulling forces allows us to include the progresses in the counterintuitive left-handed optical torque and lateral optical force as further extensions of our demonstrated pulling force, which can prove to be pivotal to the discovery of remote mass transportation, and even potentially add to the two Nobel Prizes in Physics awarded to optical force and manipulation researchers.

6.2 Summary

Over the years, as technology progressed, more and more fields of research on optics have opened up. Ever since tractor beams were first discovered in the early 1930s, it has come a long way. Today, with the help of modern technology and tools at our disposal, we can use the mechanical properties of light to guide, control, and manipulate objects on micro, nano and even atomic levels, according to user defined parameters and requirements. As research has progressed in the field of optics, so has its potential, and in our research, we have used the knowledge of optics to observe how an optical tractor beam – composed of the superposition of two electromagnetic waves (whose energy is spatially concentrated) also known as Surface Plasmon Polariton (SPP) waves – can exert a pulling force on spherical nanoparticles belonging to dielectric, chiral and plasmonic natures. Our research enabled us to study and present how the optical tractor beam composed of the two confined SPP waves was excited over the on-chip base with the help of a beam of plane polarized light propagating on to the base vertically upwards from underneath it and hitting the center of the lower dielectric substrate before travelling through to the center of the upper plasmonic substrate. The two arrays, each made of gold (Au) and comprised of 30 nano slit-like structures – gradually rotating at increased angles from top to bottom – called metasurfaces, played a crucial role in manipulating the propagating surface waves. We observed that in order to demonstrate a pulling force exerted on the spherical nanoparticle lying atop the base, the incident beam of plane polarized light had to be of a non-paraxial nature, or in other words the beam had to be perpendicular to the axis of our optical system. Although the incident beam of plane polarized light being of a non-paraxial nature is a hypothetical requirement, this issue can be addressed and counteracted upon by creating an interference field, which can be formed by the superposition of the SPP waves along with the induced effect within the spherical nanoparticle and the substrate, as a result of which the backward pulling force was realized. This backward pulling force was obtained within a certain diameter range (the Mie range) of the spherical nanoparticle.

For our research, we proposed and simulated a design for on chip configuration which consisted of a meta surface – for generating non-paraxial surface waves – as well as a surface plasmon polariton (SPP) – which has the ability to direct light in the sub wavelength scale and allowed for the possibility to realize a pulling force on all objects, with all objects being spherical nanoparticles having dielectric, plasmonic and chiral properties. Our substrate consisted of two arrays made of gold (Au) and spaced $\lambda_{SPP}/2$ apart, each having 30 nanostructures known as metasurfaces. All the nanostructures on both arrays were gradually rotated at increasing angles from top to bottom, which allowed for the generation of a pair of SPP waves on the gold surface of the chip. An incident beam of plane polarized light was also directed vertically upwards from underneath the chip so that it hit the center of the lower dielectric substrate first and then the center of the upper plasmonic substrate, in order to facilitate the generation of the SPP waves. The SPP waves were also superposed with the induced effect within the spherical nanoparticle and the substrate, which created an interference field in the y direction. The SPP waves propagating in the x direction, the interference pattern created in the y direction and the decaying in the z direction created a source of SPP cosine beam. The metasurfaces on the chip allowed for the amplitude and phase of surface waves to be controlled in such a way that the exerted SPP waves were made able to pull all objects on the chip towards the source of radiation.

During the course of our research, we designed our configuration and carried out simulations on Comsol Multiphysics, and verified our findings by running the simulations again on Lumerical FDTD. Our design consisted of a plasmonic substrate at the top having a thickness of $100x10^{-9}$ m, which was placed over a dielectric substrate at the bottom having a thickness of $200x10^{-9}$ m. Both substrates were placed in the air medium, and had widths of $11.2x10^{-6}$ m and $3.2x10^{-6}$ m respectively. A spherical nanoparticle was also placed slightly above the plasmonic substrate, with the vertical gap between the particle and the substrate being $30x10^{-9}$ m. There were also two arrays consisting of 30 nano slits each for a total of 60 nano slits on our chip, which were rotated at angles gradually increasing from top to bottom. This arrangement of the two arrays of nano slits enabled the two waves to get excited and launched with an angle θ both below and above the horizontal from the top and bottom regions of the arrays. The angular difference between the two arrays of nano slits on the chip was set at $\frac{\pi}{2}$ in order to maintain a constant magnitude across the two arrays.

The horizontal distance between the particle and the midpoint of the metasurface arrays was set at $1.5x10^{-6}$ m. Using the tools built in to Comsol Multiphysics, we changed the surface material and material property of the spherical nanoparticle between dielectric, plasmonic and chiral natures. The beam of plane polarized light hitting the chip vertically upwards from underneath the substrates created a surface wave SPP on the upper plasmonic substrate at its metal-dielectric interface. The two arrays of metasurfaces on the chip enabled the modulation of both the phase and the amplitude of the generated SPP waves. This made the SPP waves non paraxial enough so that they could pull the object towards the radiation source.

After running multiple simulations on our chip where an incident beam of plane polarized light travelling vertically upwards struck the center of the lower dielectric substrate first and then the center of the upper plasmonic substrate from below, and by varying the diameter of the dielectric, plasmonic and chiral nanospherical particle on both Comsol Multiphysics and Lumerical, we observed that non-paraxial SPP waves exerted optical pulling forces for all three particle types over a certain diameter range – the Mie range.

REFERENCES

1. Neuman, K. C., & Nagy, A. (2008). Single-molecule force spectroscopy: optical tweezers, magnetic tweezers and atomic force microscopy. Nature methods, 5(6), 491.
2. Demergis, V., & Florin, E. L. (2012). Ultrastrong optical binding of metallic nanoparticles. Nano letters, 12(11), 5756-5760.
3. Righini, M., Volpe, G., Girard, C., Petrov, D., & Quidant, R. (2008). Surface plasmon optical tweezers: tunable optical manipulation in the femtonewton range. Physical review letters, 100(18), 186804.
4. Chan, J., Alegre, T. M., Safavi-Naeini, A. H., Hill, J. T., Krause, A., Gröblacher, S., Painter, O. (2011). Laser cooling of a nanomechanical oscillator into its quantum ground state. Nature, 478(7367), 89.
5. Gao DL, Ding WQ, Nieto-Vesperinas M, Ding XM, Rahman M *et al*. Optical manipulation from the microscale to the nanoscale: fundamentals, advances, and prospects. *Light Sci Appl* 2017; **6**: e17039.
6. Ashkin, A. (1970). Acceleration and trapping of particles by radiation pressure. Physical review letters, 4(4), 156.
7. Neuman, K. C., & Nagy, A. (2008). Single-molecule force spectroscopy: optical tweezers, magnetic tweezers and atomic force microscopy. Nature methods, 5(6), 491.
8. Demergis, V., & Florin, E. L. (2012). Ultrastrong optical binding of metallic nanoparticles. Nano letters, 12(11), 5756-5760.
9. Hoeb, M., Rädler, J. O., Klein, S., Stutzmann, M., & Brandt, M. S. (2007). Light-induced dielectrophoretic manipulation of DNA. Biophysical journal, 93(3), 1032-1038.
10. Ashkin, A., & Dziedzic, J. M. (1987). Optical trapping and manipulation of viruses and bacteria. Science, 235(4795), 1517-1520.
11. F. M. Fazal and S. M. Block, “Optical tweezers study life under tension,” Nat. Photonics 5, 318–321 (2011).
12. Hoeb, M., Rädler, J. O., Klein, S., Stutzmann, M., & Brandt, M. S. (2007). Light-induced dielectrophoretic manipulation of DNA. Biophysical journal, 93(3), 1032-1038.
13. Ashkin, A., & Dziedzic, J. M. (1987). Optical trapping and manipulation of viruses and bacteria. Science, 235(4795), 1517-1520.
14. F. M. Fazal and S. M. Block, “Optical tweezers study life under tension,” Nat. Photonics 5, 318–321 (2011).
15. Qiu, C. W., Ding, W., Mahdy, M. R. C., Gao, D., Zhang, T., Cheong, F. C., Lim, C. T. (2015). Photon momentum transfer in inhomogeneous dielectric mixtures and induced tractor beams. Light: Science & Applications, 4(4), e278.

16. Chen, J., Ng, J., Lin, Z., & Chan, C. T. (2011). Optical pulling force. Nature photonics, 5(9), 531.
17. Dogariu, Aristide, Sergey Sukhov, and José Sáenz. "Optically induced'negative forces'." *Nature Photonics* 7.1 (2013): 24-27.
18. Chen, Huajin, et al. "Fano resonance-induced negative optical scattering force on plasmonic nanoparticles." *ACS nano* 9.2 (2015): 1926-1935.
19. Sukhov, Sergey, and Aristide Dogariu. "Negative nonconservative forces: optical “tractor beams” for arbitrary objects." *Physical review letters* 107.20 (2011): 203602.
20. Yevick, Aaron, David B. Ruffner, and David G. Grier. "Tractor beams in the Rayleigh limit." *Physical Review A* 93.4 (2016): 043807.
21. Novitsky, Andrey, Cheng-Wei Qiu, and Haifeng Wang. "Single gradientless light beam drags particles as tractor beams." *Physical review letters* 107.20 (2011): 203601.
22. Novitsky, Andrey, and Cheng-Wei Qiu. "Pulling extremely anisotropic lossy particles using light without intensity gradient." *Physical Review A* 90.5 (2014): 053815.
23. Chen, Jun, et al. "Optical pulling force." *Nature photonics* 5.9 (2011): 531-534.
24. Burkhartsmeyer, Jeffrey, et al. "Optical trapping, sizing, and probing acoustic modes of a small virus." *Applied Sciences* 10.1 (2020): 394.
25. Volpe, Giovanni, et al. "Surface plasmon radiation forces." *Physical review letters* 96.23 (2006): 238101.
26. Quidant, Romain, and Christian Girard. "Surface-plasmon-based optical manipulation." *Laser & Photonics Reviews* 2.1-2 (2008): 47-57.
27. Xu, Hongxing, and Mikael Käll. "Surface-plasmon-enhanced optical forces in silver nanoaggregates." *Physical review letters* 89.24 (2002): 246802.
28. Epstein, Itai, and Ady Arie. "Arbitrary bending plasmonic light waves." *Physical review letters* 112.2 (2014): 023903.
29. Lee, Wai-Hon. "Binary computer-generated holograms." *Applied Optics* 18.21 (1979): 3661-3669.
30. Epstein, Itai, and Ady Arie. "Dynamic generation of plasmonic bottle-beams with controlled shape." *Optics Letters* 39.11 (2014): 3165-3168.
31. Epstein, Itai, Yigal Lilach, and Ady Arie. "Shaping plasmonic light beams with near-field plasmonic holograms." *JOSA B* 31.7 (2014): 1642-1647.
32. Huidobro, Paloma A., et al. "Transformation optics for plasmonics." *Nano letters* 10.6 (2010): 1985-1990.
33. Della Valle, Giuseppe, and Stefano Longhi. "Graded index surface-plasmon-polariton devices for subwavelength light management." *Physical Review B* 82.15 (2010): 153411.

34. Zentgraf, Thomas, et al. "Plasmonic luneburg and eaton lenses." *Nature nanotechnology* 6.3 (2011): 151-155.
35. Li, L., et al. "Plasmonic Airy beam generated by in-plane diffraction." *Physical review letters* 107.12 (2011): 126804.
36. Evlyukhin, A. B., et al. "Splitting of a surface plasmon polariton beam by chains of nanoparticles." *Applied Physics B* 84.1-2 (2006): 29-34.
37. Drezet, Aurelien, et al. "Plasmonic crystal demultiplexer and multiports." *Nano letters* 7.6 (2007): 1697-1700
38. Avayu, Ori, et al. "Polarization controlled coupling and shaping of surface plasmon polaritons by nanoantenna arrays." *Optics Letters* 40.7 (2015): 1520-1523.
39. Lin, Jiao, et al. "Polarization-controlled tunable directional coupling of surface plasmon polaritons." *Science* 340.6130 (2013): 331-334.
40. N. Yu, P. Genevet, F. Aieta, M. A. Kats, R. Blanchard, G. Aoust, J. Tetienne, Z. Gaburro, and F. Capasso, "Flat optics: controlling wavefronts with optical antenna metasurfaces," IEEE J. Sel. Top. Quantum Electron. **19**(3), 4700423 (2013).
41. A. V. Kildishev, A. Boltasseva, and V. M. Shalaev, "Planar photonics with metasurfaces," Science **339**(6125), 1232009 (2013).
42. Y. Ling, L. Huang, W. Hong, T. Liu, L. Jing, W. Liu, and Z. Wang, "Polarization-switchable and wavelength-controllable multi-functional metasurface for focusing and surface-plasmon-polariton wave excitation," Opt. Express 25, 29812-29821 (2017).
43. Lee, Seung-Yeol, et al. "Plasmonic meta-slit: shaping and controlling near-field focus." *Optica* 2.1 (2015): 6-13.
44. Song, E. Y., Lee, S. Y., Hong, J., Lee, K., Lee, Y., Lee, G. Y., & Lee, B. (2016). A double-lined metasurface for plasmonic complex-field generation. Laser & Photonics Reviews, 10(2), 299-306.
45. Maier, S. A. (2007). Plasmonics: fundamentals and applications. Springer Science & Business Media.
46. M. R. C. Mahdy, T. Zhang, S. C. Das, and H. M. Rivy, "On chip optical tractor beam by surface plasmon polariton," Opt. Commun. 463, 125395(2020).
47. Mahdy, M. R. C., Zhang, T., Danesh, Md., Ding,W. "Substrate and Fano Resonance Effects on the Reversal of Optical Binding Force between Plasmonic Cube Dimers," Scientific reports, 7, 1: 6938 (2017).
48. Satter, S.S., Mahdy, M.R.C., Ohi, M.A.R., Islam, F. and Rivy, H.M. "Plasmonic Cube Tetramers over Substrates: Reversal of Binding Force as the Effect of Fano Resonance and Light Polarization". The Journal of Physical Chemistry C, 122, 20923-20934 (2018).

49. Rivy, H.M., Mahdy, M.R.C., Jony, Z.R., Masud, N., Satter, S.S. and Jani, R. “Plasmonicor dielectric dimers: A generic way to control the reversal of near field optical binding force”. Optics Communications, 430, 51-62 (2019).
50. Mahdy, M.R.C., Danesh, M., Zhang, T., Ding, W., Rivy, H.M., Chowdhury, A.B. and Mehmood, M.Q. Plasmonic Spherical Heterodimers: Reversal of Optical Binding Force Based on the Forced Breaking of Symmetry. Scientific reports, 8, 3164 (2018).
51. Zhu, T., Novitsky, A., Cao, Y., Mahdy, M. R. C., Wang, L., Sun, F., ... & Ding, W. (2017). Mode conversion enables optical pulling force in photonic crystal waveguides. Applied Physics Letters, 111(6), 061105.
52. Radescu, E. E. & Vaman, G. Exact calculation of the angular momentum loss, recoil force, and radiation intensity for an arbitrary source in terms of electric, magnetic, and toroid multipoles. Phys. Rev. E 65, 046609 (2002).
53. Barnett, S. M. & Loudon, R. On the electromagnetic force on a dielectric medium. J. Phys. B 39, 671–684 (2006).
54. Nieto-Vesperinas, M., Saenz, J. J., Go´mez-Medina, R. & Chantada, L. Optical forces on small magnetodielectric particles. Opt. Express 18, 11428–11443 (2010).
55. Chaumet, P. C. & Rahmani, A. Electromagnetic force and torque on magnetic and negative index scatterers. Opt. Express 17, 2224–2234 (2009).
56. Gao, D. & Shi, Ran & Huang, Yang & Ni, W. & Gao, Lei. (2017). Fano-enhanced pulling and pushing optical force on active plasmonic nanoparticles. Physical Review A. 96. 10.1103/PhysRevA.96.043826.
57. B. A. Kemp, T. M. Grzegorczyk, and J. A. Kong, "Lorentz Force on Dielectric and Magnetic Particles," J. Electromagn. Waves Appl. **20**(6), 827-839 (2006).
58. B. A. Kemp, T. M. Grzegorczyk, and J. A. Kong, "Optical Momentum Transfer to Absorbing Mie Particles," Phys. Rev. Lett. **97**(13), 133902 (2006).
59. Gansel, Justyna K., et al. "Gold helix photonic metamaterial as broadband circular polarizer." *Science* 325.5947 (2009): 1513-1515.
60. Wu, Chao, et al. "Theory and experimental realization of negative refraction in a metallic helix array." *Physical review letters* 105.24 (2010): 247401.
61. Soukoulis, Costas M., and Martin Wegener. "Past achievements and future challenges in the development of three-dimensional photonic metamaterials." *Nature photonics* 5.9 (2011): 523-530.
62. Wu, Chao, et al. "Metallic helix array as a broadband wave plate." *Physical review letters* 107.17 (2011): 177401.
63. Staelin, David H., Ann W. Morgenthaler, and Jin Au Kong. *Electromagnetic waves*. Pearson Education India, 1994.
64. Ding, K.; Ng, J.; Zhou, L.; Chan, C. T. Realization of optical pulling forces using chirality. Phys. Rev. A 2014, 89, 063825.

65. Lipkin, Daniel M. "Existence of a new conservation law in electromagnetic theory." *Journal of Mathematical Physics* 5.5 (1964): 696-700.
66. Tang, Yiqiao, and Adam E. Cohen. "Optical chirality and its interaction with matter." *Physical review letters* 104.16 (2010): 163901.
67. Bliokh, Konstantin Y., and Franco Nori. "Characterizing optical chirality." *Physical Review A* 83.2 (2011): 021803.
68. A. Lakhtakia, Selected Papers on Natural Optical Activity (SPIE Optical Engineering Press, Bellingham, WA, 1990); A. H. Sihvola, A. J. Viitanen, I. V. Lindell, and S. A. Tretyakov, Electromagnetic Waves in Chiral and Bi-Isotropic Media (Artech House, London, 1994); A. Serdyukov et al., Electromagnetics of Bi-anisotropic Materials: Theory and Applications (Gordon and Breach, Philadelphia, PA, 2001); T. G. Mackay and A. Lakhtakia, Prog. Opt. 51, 121 (2008).
69. Ng, Jack, et al. "Photonic clusters formed by dielectric microspheres:Numerical simulations. “Physical Review B 72.8 (2005): 085130.
70. Novitsky, A., Gao, D., Gorlach, A. A., Qiu, C. W., & Lavrinenko, A. V. (2017, July). Non-diffractive tractor beams. In 2017 19th International Conference on Transparent Optical Networks (ICTON) (pp. 1-4). IEEE.
71. Zhang, P., Prakash, J., Zhang, Z., Mills, M. S., Efremidis, N. K., Christodoulides, D. N., & Chen, Z. (2011). Trapping and guiding microparticles with morphing autofocusing Airy beams. Optics letters, 36(15), 2883-2885.
72. Ruffner, D. B., & Grier, D. G. (2012). Optical conveyors: a class of active tractor beams. Physical review letters, 109(16), 163903.
73. Punzmann, H., Francois, N., Xia, H., Falkovich, G., & Shats, M. (2014). Generation and reversal of surface flows by propagating waves. Nature Physics, 10(9), 658.
74. Gao, D., Ding, W., Nieto-Vesperinas, M., Ding, X., Rahman, M., Zhang, T.,Qiu, C. W. (2017). Optical manipulation from the microscale to the nanoscale: fundamentals, advances and prospects. Light: Science & Applications, 6(9), e17039.
75. Gorlach, A. A., Gorlach, M. A., Lavrinenko, A. V., & Novitsky, A. (2017). Matter-wave tractor beams. Physical review letters, 118(18), 180401.
76. Zhu, T., Mahdy, M. R. C., Cao, Y., Lv, H., Sun, F., Jiang, Z., & Ding, W. (2016). Optical pulling using evanescent mode in sub-wavelength channels. Optics express, 24(16), 18436-18444.
77. Dogariu, A., Sukhov, S., & Sáenz, J. (2013). Optically induced'negative forces'. Nature Photonics, 7(1), 24.
78. Arlt, J., & Dholakia, K. (2000). Generation of high-order Bessel beams by use of an axicon. Optics Communications, 177(1-6), 297-301.
79. Turunen, J., Vasara, A., & Friberg, A. T. (1988). Holographic generation of diffraction-free beams. Applied Optics, 27(19), 3959-3962.

80. McGloin, D., & Dholakia, K. (2005). Bessel beams: diffraction in a new light. Contemporary Physics, 46(1), 15-28.
81. Brzobohatý, O., Karásek, V., Šiler, M., Chvátal, L., Čižmár, T., & Zemánek, P. (2013). Experimental demonstration of optical transport, sorting and self-arrangement using a ‘tractor beam’. Nature Photonics, 7(2), 123.
82. Petrov, M. I., Sukhov, S. V., Bogdanov, A. A., Shalin, A. S., & Dogariu, A. (2016). Surface plasmon polariton assisted optical pulling force. Laser & Photonics Reviews, 10(1), 116-122.
83. Zayats, A. V., Smolyaninov, I. I., & Maradudin, A. A. (2005). Nano-optics of surface plasmon polaritons. Physics reports, 408(3-4), 131-314.